Since January 2020 Elsevier has created a COVID-19 resource centre with free information in English and Mandarin on the novel coronavirus COVID-19. The COVID-19 resource centre is hosted on Elsevier Connect, the company's public news and information website.

Construction and Building Materials 266 (2021) 120892

Contents lists available at ScienceDirect

Construction and Building Materials

journal homepage: www.elsevier.com/locate/conbuildmat

Experimental investigation on the long-term behaviour of prefabricated timber-concrete composite beams with steel plate connections

Benkai Shi [a], Weiqing Liu [a,b,*], Huifeng Yang [b,*]

[a] School of Civil Engineering, Southeast University, Nanjing 211189, PR China
[b] College of Civil Engineering, Nanjing Tech University, Nanjing 211816, PR China

HIGHLIGHTS

- Experimental investigation under indoor environment was conducted.
- The influence of loading levels and the number of shear connections on long-term deformations.
- Long-term deflection, interface slip, and timber strain were measured and analyzed.
- Time-dependent behaviour of timber-concrete composite beams were predicted.

GRAPHICAL ABSTRACT

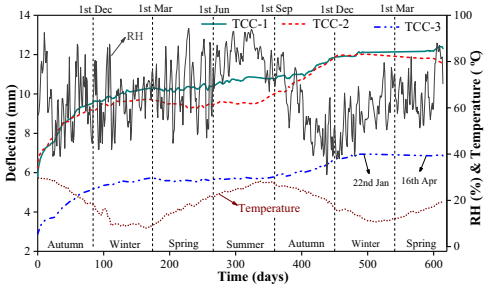

ARTICLE INFO

Article history:
Received 13 December 2019
Received in revised form 11 August 2020
Accepted 11 September 2020
Available online 1 October 2020

Keywords:
Timber-concrete composite
Prefabricated
Steel plate connection
Long-term behaviour
Interface slip
Timber structures

ABSTRACT

This paper presents the results of long-term experiments performed on three timber-concrete composite (TCC) beams. An innovative fabricated steel plate connection system, which consists of screws and steel plates embedded in concrete slabs, was adopted in the TCC beam specimens. The adopted shear connection can provide dry-type connection for TCC beams. Steel plates were embedded in concrete slabs while the concrete slab was constructed in factories. The timber beam and concrete slab can be assembled together using screws at the construction site. In this experimental programme, the beam specimens were subjected to constant loading for 613 days in indoor uncontrolled environments. The influence of long-term loading levels and the number of shear connections on the long-term performance of TCC beams was investigated and discussed. The mid-span deflection, timber strain, and interface relative slip at the positions of both connections and beam-ends were recorded throughout the long-term tests. It was found the long-term deflection of the TCC beam increased by approximately 60% while the long-term loads were doubled. Under the influence of the variable temperature and humidity, the TCC specimens with 8 shear connections showed slighter fluctuations compared with the TCC beam with 6 shear connections. In the 613-day observation period, the maximum deflection increment recorded was 6.56 mm for the specimen with eight shear connections and 20% loading level. A rheological model consisting of two Kelvin bodies was employed to fit the curves of creep coefficients. The final deflections predicted of all specimens at the end of 50-year service life were 2.1~2.7 times the initial deflections caused by the applied loads. All beam specimens showed relative small increments in mid-span deflection, strain and relative slip over time without any degradations, demonstrating the excellent long-term performance of TCC beams using the innovative steel plate connection system, which is also easily fabricated.

* Corresponding authors.
E-mail addresses: wqliu@njtech.edu.cn (W. Liu), hfyang@njtech.edu.cn (H. Yang).

https://doi.org/10.1016/j.conbuildmat.2020.120892
0950-0618/

1. Introduction

Facing with the serious pollutions brought by the industrial process, the development of green buildings and the environmental protection during construction process are critically needed. Accordingly, timber structures obtained pronounced attentions due to all kinds of advantages, such as environmental friendly, livable and assemblability [1]. In frame structure systems, the application of timber structures may be constrained due to the limitation of deflection deformation for the flexural members. An effective measure to improve the bending stiffness and load-bearing capacity of a new-built or existing timber beam is strengthening it by arranging a concrete slab/beam on the top of the timber beam [2]. In the regions highly corrosively to concrete structures, the timber floors are also applied to the bottom of concrete slabs to prevent corrosive environment from corroding the concrete [3].

The slip performance of shear connections and composite efficiency of timber-concrete composite (TCC) beams/floors have been the research topics of TCC systems. To obtain a superior composite action and structural performance, many types of shear connections have been proposed and researched. Typical shear connections include dowelled, notched, glued, and hybrid connections. Dowelled connections are characterized by the simple structure and clear stress path. The dowelled connections exhibited better shear performance by the inclination arrangement [4] and adding additional shear plate [4,5]. Sebastian et al. [6] demonstrated that screws developing tension at 45° inclination showed a 14.7% improvement of bearing capacity than vertical screws in shear connections. Khorsandnia et al. [7] discovered that the employment of bidirectional inclined screw could enhance the slip stiffness by 65.9% than the vertical screw connections. In addition, notched [8,9] and glued-in steel-plate connections [10,11] were proposed to obtain better loading-capacity and slip stiffness. Djoubissie et al. [12] found that the shear strengths and slip moduli of notched-rebar connections were improved by 40% and 5.3 times, respectively, compared with pure rebar connections. The composite efficiency of TCC floors with notched connections reached to 83.4% [13]. For the glued-in steel-plate connections, the shear bearing capacity and slip moduli were tested as 276.0 kN and 3368.4 kN/mm, respectively [14], and the composite efficiency for the TCC beams with glued-in steel-plate connections reached to 93% at the initial loading stage [15].

Apart from improving the mechanical property of TCC systems, the feasibility and convenience of construction were also the research topics in recent years. Therefore, several types of prefabricated TCC structures were proposed and investigated. Lukaszewska et al. [16,17] investigated several types of shear connections which can realise the semi-prefabrication of TCC beams. Crocetti et al. [18] proposed an effective method to realise the 'dry-dry' connection of TCC beam by using inclined screws. Khorsandnia et al. [19] also researched several possibilities for the deconstructable TCC beams, and obtained desired structural performances. Zhu et al. [20] proposed an innovative hybrid connection, which consists of steel plated pre-embedded in concrete and screws, aiming to explore the feasibility for prefabricated TCC systems. Zhang et al. [21] investigated the prefabricated TCC beam using coach screws, by embedding a wooden dowel in the concrete slab, and achieved a composite efficiency of 81.9%.

The prefabricated TCC system is characterized by the following advantages. (1) The concrete slab can be constructed in factories in advance, saving time needed for concrete to cure and costing down than traditional TCC structures which need cast concrete slabs onsite. (2) To prevent the water penetrating to timber beams, an interlayer made by plywood is necessary. It was found than the interlayer could evidently decreases the slip moduli of shear connections and bending stiffness of TCC structures [22]. (3) The prefabricated concrete slabs could reduce the high creep of concrete during curing [18]. (4) Reduce the pollution on the construction site and improve construction efficiency [23].

Because timber and concrete show different creep properties, the time-dependent behaviour of the TCC structure is more complex compared with pure timber and concrete beams. The concrete shrinks during the whole service life while timber shrinks or swells with the variation of relative humidity and temperature [24]. Therefore, many experimental investigations about time-dependent behaviours of shear connections [25–28] and TCC beams [29–32] were conducted. It was found the type and configuration of connections have a great influence on the long-term slip of composite beams [26,33]. In addition, Van de Kuilen et al. [27] investigated the effect of dimension parameter on the time-dependent behaviour of dowelled connections, and discovered that increasing the dowel diameter could decrease the creep coefficient, and the smooth dowel connection showed a minor creep coefficient than the profiled one.

Many experiments were performed to investigate the influence of concrete and shear connection types on the creep performance of TCC system [34–36]. Yeoh et al. [34] found the application of low shrinkage concrete could decline the long-term deflection by 12.8% than the specimen with normal concrete. Fragiacomo & Lukaszewska [35] investigated the long-term performance of TCC floors with prefabricated concrete slabs, which verifies the feasibility of prefabricated TCC structures. Compared with the specimen with screwed connections, the beam specimen with grooved connectors showed less creep tendency while the specimen with adhesive connection was characterized the biggest creep deformation [36]. In addition, Fragiacomo et al. [37] also demonstrated the seepage of wet concrete won't lead to a possible decay of timber while there is no plywood interlayer between the timber member and the concrete one. However, the construction methods such as casting in situ or prefabricated, shoring time and shored or unshored have pronounced influences on the time-dependent behaviour of TCC structures [38].

An innovative shear connection consisting of metal plates and screws, which can provide dry-type assembly between timber and concrete members, was demonstrated to possess excellent strength and slip moduli [20]. The TCC beam with this type of connection is verified to show excellent structural performance, which is easy to prefabrication [39]. Therefore, to further explore the feasibility of TCC systems using this type of fabricated steel plate connections, the long-term performance of TCC system with steel plate connections need to be investigated. Furthermore, as summary above, the investigations about the time-dependent behaviour of shear connections and composite beams need to be supplemented further, especially for the prefabricated TCC systems. Therefore, the primary objects of this article are to investigate the long-term performance and feasibility of the prefabricated beams using the steel plate connections. The influence of the number of shear connections and sustained loading levels coupled with the changing environmental conditions was considered in the long-term tests.

2. Beam specimens

2.1. Materials

The timber adopted in this experimental programme was made of Douglas fir glued laminated timber. The glulam was fabricated by Engineering Research Center of Modern Timber Structure Laboratory, Nanjing Tech University. The strength class of the timber

was determined as GL28h in accordance with EN 1194 [40]. The average moisture content of structural lumbers was lower than 15% while the glulam was fabricated. The main material properties of glulam parallel to the grain are displayed in Table 1. The ranges, coefficient of variation (CoV), and the number of tested samples are also displayed in Table 1. The elastic modulus E_w and bending strength f_m of glulam were tested as 12863 MPa and 30.8 MPa, respectively, according to ASTM D198 [41]. The bending strength of glulam was tested through by bending tests performed on three full-size glulam beams according to GB/T 50329 [42]. The shear and tension strengths were tested in accordance with the ISO 3347 [43] and ISO 3345 [44], respectively. The samples for testing shear and tension strengths were made of the dimension lumbers almost without defects. Therefore, their testing results were higher than the characteristic values of GL 28 h in EN 1194. The shear strength of adhesive bonds were tested as 9.9 MPa according to ASTM D905 [45]. The moisture content of the wood was tested as 10.9% in accordance with EN 13183-1 [46] while the material tests were performed.

The strength class of concrete adopted in this experimental programme was C30/35. The average cubic compressive strength was measured as 38.3 MPa after curing 28 days. The modulus of elasticity E_{cm} of concrete was evaluated as $3.3 \times 10^4 N/mm^2$ according to Eurocode 2 [47].

The coach screw diameter is 6 mm while the length is 70 mm. The bending yield strength of screws was measured as 219.6 MPa according to ASTM F1575 [48]. The withdraw capacity of the screw parallel to grain and perpendicular to grain were measured as 5.78 kN and 7.30 kN, respectively, according to EN 1382 [49].

2.2. Beam specimen description

Three TCC beams were prepared for the long-term tests. The details of the TCC beams employed in long-term tests are displayed in Fig. 1 and Table 2. The total length of beam specimens was 4800 mm, whereas their clear span during long-term loading tests was 4500 mm. Eight shear connections were used to connect the concrete slab with the timber beam for TCC-1 and TCC-3, while six ones for TCC-2. The shear connections spaced at 600 mm centers for TCC-1 and TCC-3 at each half-span, while the center distance for TCC-2 was 800 mm.

Only one specimen was prepared for each configuration. A synchronous investigation about notched-screw connections and TCC beams was reported [50], in which three push-out specimens were constructed for each loading level. It was demonstrated that the difference between each specimens can be negligible. According to existing literatures, the loading levels in long-term tests of beam specimens mostly ranged from 10% to 30% [31,35,37,50]. Thus, the lower loading levels was determined as 10% of the load-carrying capacity, which was applied to the specimen TCC-3. To investigate the influence of loading levels, the long-term loads sustained by TCC-1 and TCC-2 were about 20% of their estimated short-term load-carrying capacity. The shear connection quantity and loading levels were the main research parameters for the long-term behaviour of the composite beams.

The configuration of the fabricated shear connection is shown in Fig. 2. The cross-section dimension of the concrete slab was 400 mm width and 80 mm depth, while the cross-section dimension of the timber beam was 135 mm width and 300 mm depth. The shear connection is composed of two steel plates and sixteen screws. The details of the steel plate are displayed in Fig. 3. Two steel plates were partly embedded into the concrete slab while the concrete slab was constructed, and then laterally screwed on the timber block. Two angle steel strips were bolted on each steel plate to improve the cementation between steel plates and concrete. The strength grade of bolts adopted was grade 8.8. The dimension of the bolt is 12 mm diameter and 40 mm length. Both the steel plate and angle steel were made by S355 steel.

2.3. Short-term performance of the fabricated shear connection

The experimental outcomes of symmetrically push-out tests for the steel plate connection were reported by a previous study [20]. Typical mechanical properties for two shear planes are displayed in Table 3. The average ultimate bearing capacity of three push-out specimens was tested as 174.1 kN, while the slip modulus $K_{0.4}$ in serviceability limit state was 48.2 kN/mm. The value of $K_{0.8}$, denoting the slip modulus in ultimate limit state, only showed slight decline compared with $K_{0.4}$ and $K_{0.6}$.

Apparently, this innovative steel plate connection is characterized by acceptable strength, slip moduli, and superior ductility, coupled with good feasibility for the assembly of prefabricated members. Therefore, the long-term behaviour of prefabricated TCC structures using this steel plate connection should be evaluated to further ensure its feasibility in long-term service life.

2.4. Short-term performance of the TCC beam and simplified calculations

To determine the ballast loads in long-term tests, the simplified method based on 'γ-method' was adopted to estimate the load-carrying of TCC beam specimens as shown in the Appendix. The effective bending stiffness of a TCC beam specimen can be estimated in accordance with the 'γ -method' suggested by Eurocode 5 [51]. The calculation formula for the effective bending stiffness are displayed in Appendix Eqs. (1)–(4). Then, the mid-span deflection of TCC beam under the action of ballast loads can be estimated by Eq. (5). Through by Eq. (10), the load-carrying capacity of TCC beams can be estimated.

To demonstrate the accuracy of the simplified method in Appendix, a preliminary experimental study reported by Shi et al. [39] was cited for comparison. In addition, short-term experimental results can also provide significant information about the short-term structural performances, which is beneficial for us to realise the TCC beams with steel plate connections. The TCC beam with the total length of 6000 mm and 10 steel plate connections (center space of 630 mm) was tested in the preliminary study, and the cross-section was same as the TCC beam specimens adopted in this long-term research. The timber was made of a same batch of lumber as long-term tests, and the concrete strength class was also C30/35.

Table 1
Material properties of the adopted timber parallel to grain.

Designation	Range (MPa)	Mean values (MPa)	CoV (%)	Quantity
Elastic modulus	10521.7–14232.9	12,863	13.0	10
Compressive strength	27.8–32.4	29.4	5.1	10
Bending strength	28.2–32.1	30.8	6.0	3
Shear strength	3.1–8.9	6.1	27.5	34
Tension strength	38.8–75.9	55.8	22.6	10

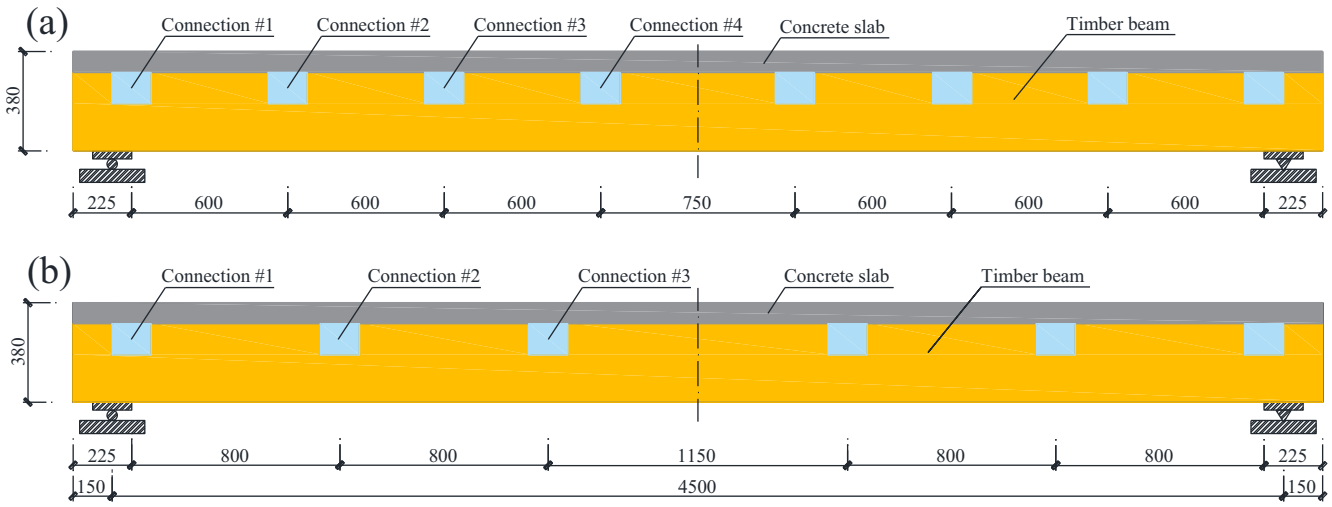

Fig. 1. Geometric details of beam specimens: (a) TCC-1 and TCC-3, (b) TCC-2 (Unit: mm).

Table 2
TCC beams employed in long-term tests.

Specimens	Number of connections	Connection distance (mm)	Loading level
TCC-1	8	600	20%
TCC-2	6	800	20%
TCC-3	8	600	10%

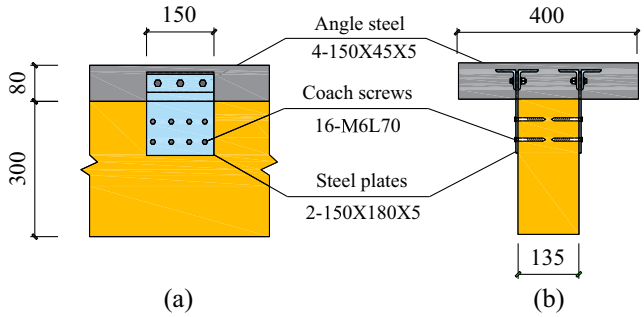

Fig. 2. Details of the shear connection: (a) front view, (b) cross-section diagram (Unit: mm).

Table 3
Mechanical properties of fabricated shear connections [20].

Properties	Values
Load-bearing capacity F_{max}	174.1 kN
Maximum slip s_{max}	13.3 mm
Slip modulus $K_{0.4}$	48.2 kN/mm
Slip modulus $K_{0.6}$	45.3 kN/mm
Slip modulus $K_{0.8}$	35.9 kN/mm

The load–deflection curve of the 6000 mm long TCC beam with steel plate connections is shown in Fig. 4. Moreover, Fig. 4 also displays the slope curves for various composition actions (including effective bending stiffness, non- and full-composite action). The bending stiffness for the TCC beam with non- and full-composite action are calculated by Appendix Eqs. (6) and (7), respectively. The slopes of the curves in Fig. 4 are calculated by the Eq. (8) in the Appendix. The composition efficiency was estimated as 72.0% according to the Eq. (9), which denotes the proposed fabricated connection can provide superior composite action for TCC systems.

The comparisons between experimental and analytical results for both effective bending stiffness and load-carrying capacity based on 'γ -method' are shown in Table 4. The analytical results for bending stiffness and load-carrying capacity were calculated

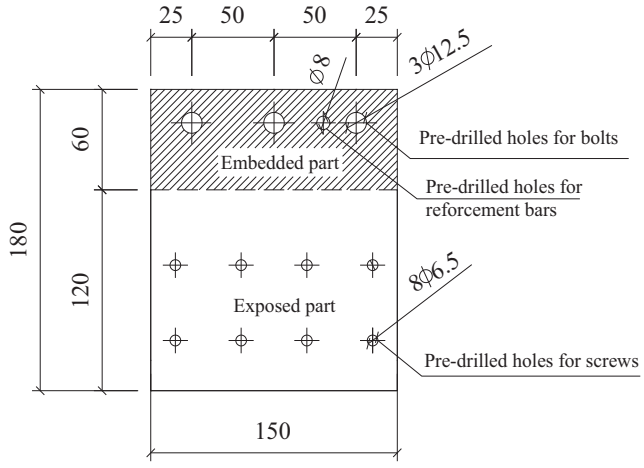

Fig. 3. Details of the steel plate (Unit: mm).

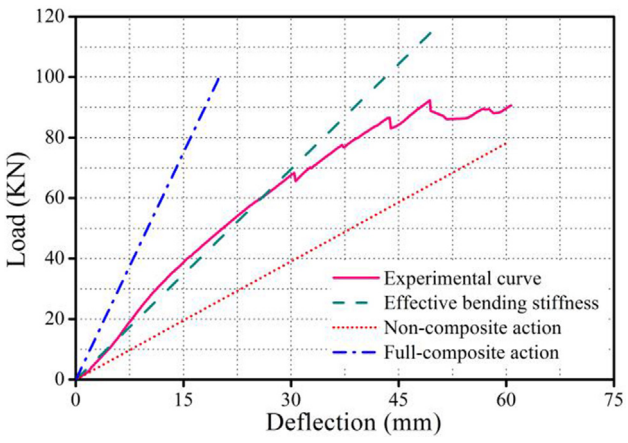

Fig. 4. The load–deflection curve of the TCC beam.

Table 4
Comparisons between experimental and analytical results [39].

Item	Bending stiffness (10^{12}N.mm^2)	Load-carrying capacity (kN)
Experimental results	9.16	87.7
Analytical results	7.62	98.2
Error	−16.8%	+12.0%

by Eq. (1) and Eq. (10), respectively. As shown in Table 4, the available analytical methods show an acceptable accuracy, which agree well the experimental results.

The available analytical methods were adopted to estimate the short-term mechanical performance of TCC beams specimens adopted in long-term tests, and the calculated outcomes are shown in Table 5. The load-carrying capacity for TCC-1(-3) and TCC-2 are 118.7 and 113.2 kN, respectively. Thus, the long-term loads for TCC-1 and TCC-2 are 24.0 and 22.8 kN, respectively, being basically 20% of their bearing capacity. The deigned long-term loads sustained by TCC-3 is 12.0 kN, which was approximately 10% estimated bearing capacity. In addition, the initial deflection was estimated as 5.75, 6.22, and 2.88 mm for specimen TCC-1, TCC-2, and TCC-3, respectively.

2.5. Test methods and devices

The timber beams were constructed on May 4, 2018. The concrete slab were constructed on May 12, 2018. The long-term loads were applied to the TCC beam specimens on September 8, 2018. The long-term test diagram and device are illustrated in Fig. 5(a), and the photograph of a tested specimen is shown in Fig. 5(b).

The long-term loads were applied at the third-span points of beam specimens as shown in Fig. 5(a). Long-term loads consisted of concrete and steel weights. The long-term tests were conducted inside the basement of the structural laboratory of Nanjing Tech University. The surrounding environment of beam specimens was uncontrolled and variable. The indoor conditions can protect the specimens and testing instruments from strong winds and heavy rainfall, thereby ensure the accuracy of experimental data. However, the RH and temperature in sheltered indoor environment fluctuated more slightly than the outdoor conditions.

Long-term tests were started on 8th September 2018, which has been carried out for 613 days while this article was submitted. It is sufficient to reflect the effect of long-term loads and seasonal environmental changes on the deformations of TCC specimens in terms of loading time. Following variables were recorded over time during the entire period of loading tests. (1) Initial mid-span deflections. (2) RH and temperature of surrounding air; (3) The increase in mid-span deflection; (4) Relative slip at both beam-ends and the positions of shear connections; (5) Strains of the bottom of timber beam at third-span points. The RH and temperature were recorded once per hour by a temperature and humidity sensor. All deformations were monitored by dial gauges with the accuracy of 0.01 mm. The dial gauges were installed ahead before the concentrated loadings were applied. The initial deformations were measured immediately after the loads were applied (all weight blocks were applied in 15 min). The gauge data were recorded manually. The dial gauges measuring the mid-span deflection, the slip at beam ends, and timber strains were shown in Fig. 5 (a). The timber strains were evaluated through by measuring the relative deformation of a 200 mm interval. The relative slip of shear connections was measured by dial gauges which were fixed at the positions of shear connections. All deformations were recorded once per hour in the former 12 h, and then be obtained daily basically. The long-term tests are still on-going while authors submitted this manuscript.

Table 5
Estimated short-term performances and long-term loads of TCC beam specimens.

Items	TCC-1	TCC-2	TCC-3
Estimated bearing capacity, $2P_{max}$ (kN)	118.7	113.2	118.7
Effective bending stiffness, $(EI)_{eff}$ (10^{12}N.mm^2)	6.75	6.18	6.75
Long-term loads, $2P$ (kN)	24.0	22.8	12.0
Self-weight, q (kN/m)	1.2	1.2	1.2
Initial deflection, w_0 (mm)	5.75	6.22	2.88

3. Experimental results

3.1. Initial deflection, surrounding RH and temperature

The comparisons between measured and estimated values are displayed in Table 6. The estimated values are basically consistent with the measured values, which demonstrated the reliability of the estimated calculation method. The measured values for TCC-1 and TCC-2 were 10%~12% smaller than estimated ones, while the measured value of TCC-3 was 7% bigger than its estimated value. Apparently, the measured values exhibited an evident fluctuation by comparing TCC-1 and TCC-3. While the ballast loads were doubled, the measured deflection of TCC-1 only increased by 63.6% compared with that of TCC-3. However, it was supposed that the deflection of the TCC beam linearly increased corresponding to loads while the loads were less than 30% of load-carrying capacity [16]. The load–deflection curve in Fig. 4 also demonstrated this conclusion. The fluctuation of the deflection was caused by the vibrations and irregularity during the process of applying concrete and steel weights. Therefore, the displayed data of dial gauges immediately caused by the applied loads was not recommended to determine the initial deformations [50,52]. The initial deformations estimated by simplified methods are employed to calculate the creep coefficient as follows [28]:

$$\varphi(t) = \frac{v(t) - v(t_0)}{v(t_0)} \tag{11}$$

where, v denotes possible deformations (mid-span deflections in this article); t_0 and t signify the initial time of long-term load application and the current time, respectively.

The recorded temperature and RH during the entire recorded testing period are plotted in Fig. 6 coupled with deformation data. The temperature ranged from 8.2 °C–30.4 °C, while the RH ranged from 31.1%–94.3%. The temperature showed obvious seasonal variation, reaching the minimum value in the winter and peaking in the summer. In addition, the relative humidity also certain evident periodical changes. However, the RH maintained relative high values most of the time due to the rainy climate of Nanjing city. From about 350 to 450 days, the RH exhibited the relatively low period due to the long period of dry weather. This climate condition is valuable to investigate the influence of long-term extreme environmental conditions on the deformation of TCC beams. Combining the recorded temperature and humidity curves, the creep tendencies of composite beams are analyzed hereinafter in mid-span deflections, timber strains and interface slips.

3.2. Mid-span deflections

The measured mid-span deflections of all specimens are depicted in Fig. 6. Based on the estimates values shown in Table 5, the initial mid-span deflections in Fig. 6 were 5.75 mm for TCC-1, 6.22 mm for TCC-2 and 2.88 mm for TCC-3. Results in Fig. 6 show the deflections evidently increased in the former 120 days, and

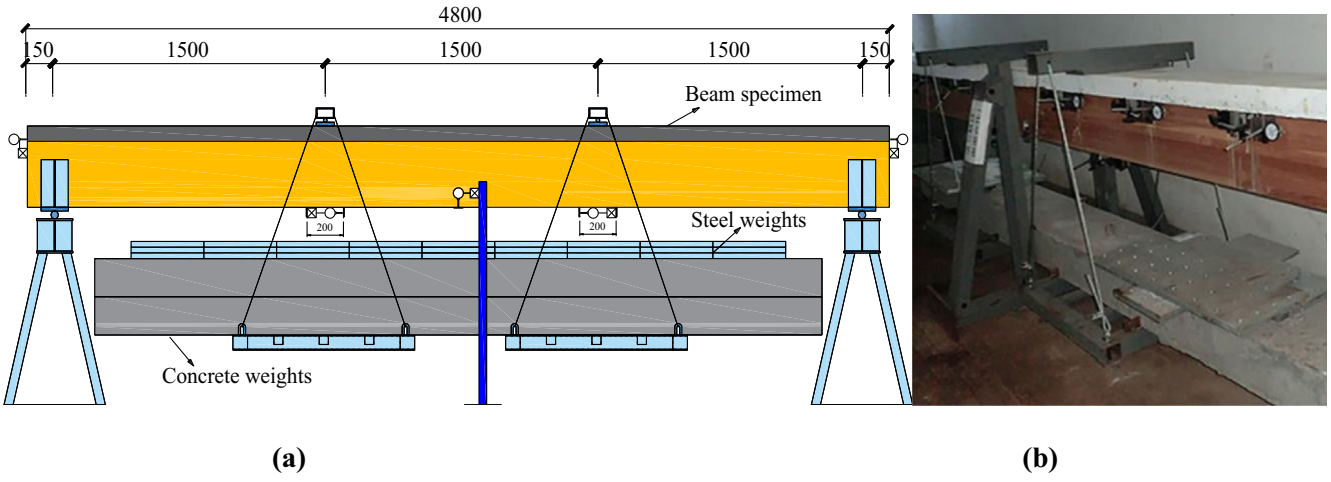

Fig. 5. Long-term loading diagram: (a) elevation (Unit: mm), (b) the photo of a tested specimen.

Table 6
Comparisons between measured and estimated values for initial mind-span deflections (Unit: mm).

Specimens	Measured values	Estimated values
TCC-1	5.04	5.75
TCC-2	5.58	6.22
TCC-3	3.08	2.88

then tended to stabilization with negligible fluctuations. The increase of deflection in the first 120 days was dominantly contributed by the creep deformation caused by the action the long-term loads. From approximately 330 to 450 days, the decrease of both temperature and RH caused the increase in mid-span deflection. During this period, the RH dropped to 31.1% from 84.9%, whereas the temperature declined to 19.9 °C from 27.2 °C. All specimens tended to stabilization again with the increase of RH approximately from 1st December 2019, and two specimens (TCC-2 and TCC-3) occurred slight decline in the spring of 2020 due to increase of RH and temperature. Due to the impact of COVID-19, the recording was suspended on January 22 and restarted on April 16, 2020.

Table 7 displays the increase in mid-span deflection at some key times, where Dec 1, 2018, Mar 1, Jun 1, Sep 1, and Dec 1, 2019 are the dates expressed by the vertical dash lines in Fig. 6 from left to right, respectively. The long-term deflections increased by 54.8% to 90.6% in the former 120 days compared with initial deflections. From Mar 1 to Sep 1, 2019, the long-term deflections increase slowly, and for the TCC-2 and -3, the deflection even declined, which was caused by the high values of the RH and temperature. The deflections also increased obviously from Sep 1 to the Dec 1, 2019. From Dec 1, 2019 (the 449th day) to the 613th day, the deflection of each specimen increased slightly, and even decreased in the spring of 2020. At the end of recorded dates, the deflection increments were 6.56 mm, 5.35 mm, and 3.97 mm, respectively, for specimens TCC-1, TCC-2, and TCC-3, which are the 114.1%, 86.0%, and 137.8% of corresponding initial deflections.

By comparing the specimen TCC-1 with TCC-3, it can be concluded that the long-term deflection increased by approximately 60% while the applied concentrated loads were doubled. Therefore, with the increase the load level, the creep coefficient will decline. The increase in deflection of TCC-2 was slightly smaller than that of TCC-1, which was contrary to the expectation. This may be caused by the material differences among each beam component,

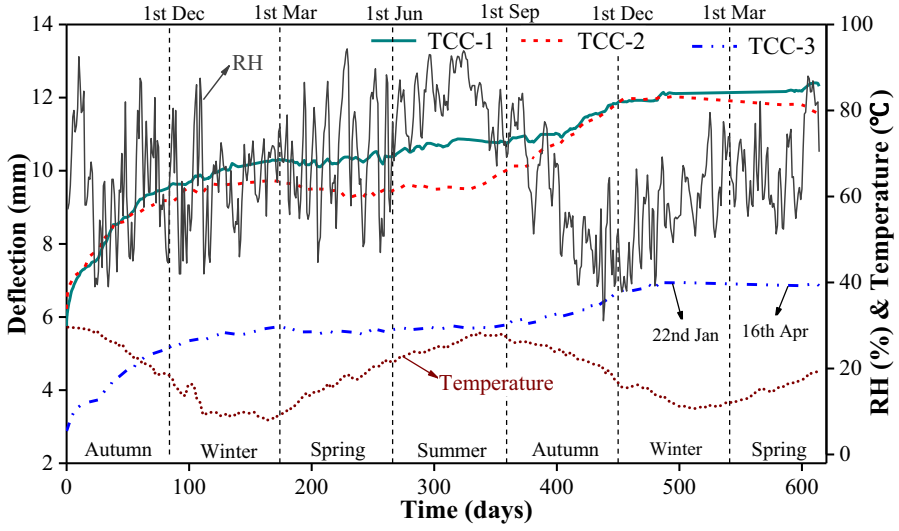

Fig. 6. Mid-span deflections of all specimens.

Table 7
The increase in mid-span deflection at some key times.

Key times (days)	TCC-1		TCC-2		TCC-3	
	Δw (mm)	$\Delta w/w_0$	Δw (mm)	$\Delta w/w_0$	Δw (mm)	$\Delta w/w_0$
Initial deflection, w_0 (mm)	5.75		6.22		2.88	
1st day	0.47	8.2%	0.50	8.0%	0.16	5.6%
10th day	1.39	24.2%	1.01	16.2%	0.68	23.6%
50th day	3.01	52.3%	2.54	30.8%	1.64	56.7%
Dec 1, 2018 (84th day)	3.87	67.3%	2.97	47.7%	2.32	80.6%
120 days	4.21	73.2%	3.41	54.8%	2.61	90.6%
Mar 1, 2019 (174th day)	4.54	79.0%	3.46	55.6%	2.84	98.6%
Jun 1, 2019 (266th day)	4.63	80.5%	3.26	52.4%	2.78	96.5%
Sep 1, 2019 (358th day)	5.00	87.0%	3.82	61.4%	2.89	100.3%
Dec 1, 2019 (449th day)	6.16	107.1%	5.67	91.1%	3.83	133.0%
500th day	6.36	110.6%	5.79	93.1%	4.06	140.9%
613th day	6.56	114.1%	5.35	86.0%	3.97	137.8%

and the structural performance difference between TCC-1 and TCC-2 was relatively small. However, the TCC-2 exhibited a more obvious increase while the RH and Temperature decreased after Sep 1, 2019. This can be explained that the TCC with less shear connections is more sensitive to the surroundings temperature and RH. This is because that the bending stiffness and the composite action declined with the decrease of the shear connections. With the obviously decrease of RH, the creep deformation of concrete slabs increased during the long-term loading. The specimen TCC-1 showed superior capacity of constraining creep deformation than TCC-1, thanks to more shear connections and greater flexural stiffness.

3.3. Strains of timber components

The creep tendencies of timber strains at the third-span points are depicted in Fig. 7. The strain tendencies of TCC-1 and TCC-2 were basically similar throughout the entire record duration. The timber strain linearly increased under the action of applied loads in the first 18 days, and then experienced the decline phase (20 to 60 days) and fluctuation stages (60 to 170 days). The timber strain increased during the sorption phase due to the high RH from approximately 170 days to 340 days, and then decreased during the desorption phase from approximately 380 days to 440 days. The initial of timber strain TCC-3 basically kept the increase tendency in the first 170 days, and also increased with the increase of RH and decreased with the reduction of RH from the 300th to 440th day. From about 440 days to 613 days, the strain of timber basically showed an increase tendency due to the RH recovered to relatively high levels. The peaking values of timber strain for TCC-1, TCC-2, and TCC-3 were reached as 1045, 1010, and 490 με, respectively.

Comparing Fig. 7 with Fig. 6, the timber strain was characterized by obvious fluctuations while compared with the mid-span deflection. Apparently, the changing RH and temperature have a more pronounced influence on the micro deformation than the structural macro response. In addition, the strain tendency of the timber showed the retardation phenomenon, while compared with the tendency of RH. As shown in Fig. 7, the overall trend of RH began to decrease at about the 320th, whereas the timber strain began to decline at the 380th day for TCC-1, the 340th day for TCC-2, and the 405th day for TCC-3.

3.4. Interface relative slips

Interface relative slips at the positions of both beam-ends and shear connections are depicted in Figs. 8–10. By comparing the slip curves in Figs. 8–10, the slip of TCC-1 was the biggest, TCC-2 was less, and TCC-3 was the least for most of record time. And the slip of the innermost shear connections was the smallest, whereas the slip of connection #2 are the biggest. Main discoveries can be obtained as follows: (1) Most curves showed an increase tendency in the first 80 days, and then basically stabilised, except the connection #2 and #3 in TCC-1 and connection #2 in TCC-3, which almost have been increasing during the whole long-term tests. (2) The long-term slips of beam-ends were smaller than those of connections #2 and #3 for TCC-1 and TCC-3, and connection # 2 for TCC-2. (3) The variable RHs have a more pronounced effect on the relative slip at the beam-ends than that at shear connections. Accordingly, the fluctuation amplitude of relative slip at the positions of shear connections were much slighter than that at beam-ends. (4) The long-term slip showed an obvious descent stage from approximately 10th to the 25th day, while the RH declined abruptly, which is consistent with the strain of timber in Fig. 7.

4. Discussions

4.1. Creep coefficients

The creep coefficient reflects the relative deformation corresponding to the initial deformation, and has been widely used to describe the creep behaviours of timber beams [53] and TCC connections [28]. The creep coefficients of mid-span deflections for all specimens were calculated according to Eq. (11), and the curves of creep coefficients were plotted in Fig. 11.

As shown in Fig. 11, specimen TCC-3 showed the biggest values of creep coefficient in the later stage of long-term tests, TCC-1 took the second place, and the creep coefficient of TCC-2 was the smallest. The creep coefficient of TCC-3 showed the approximately 20% enhance than that of TCC-1. The reason leading to the biggish values of creep coefficient for TCC-3 is that its estimated initial deflection is just 50% of TCC-1, while its long-term deformation increment was about 0.6 time that of TCC-1. The TCC-2 showed the smallest creep coefficient as the result of minor deformation compared with TCC-1 and the biggest initial deflection among all three specimens. The creep coefficient values at different key times are shown in Table 7, the creep coefficient decreased with increase of applied loads.

A rheological model consisting of two Kelvin bodies can be used to fit the creep coefficient curves [28]. The constitutive model of two Kelvin bodies can be expressed by Eq. (12). This model doesn't precisely consider the effect of variations of temperature, RH and moisture content of component materials. However, the environmental temperature and RH showed seasonal fluctuations, leading to the slightly seasonal fluctuations of the deflections [33,36], which was also reflected in Fig. 11. It has been demonstrated that the long-term deflection fluctuated around the fitting curves sim-

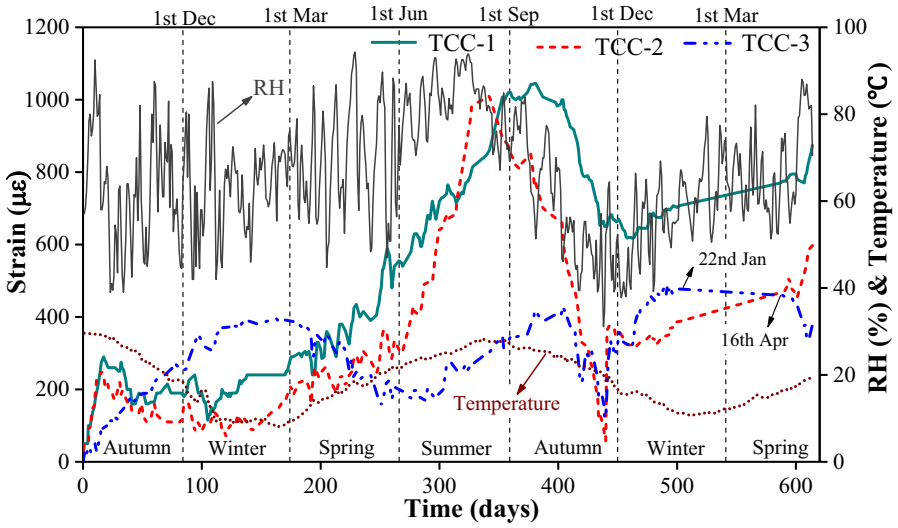

Fig. 7. Strains of timber beams.

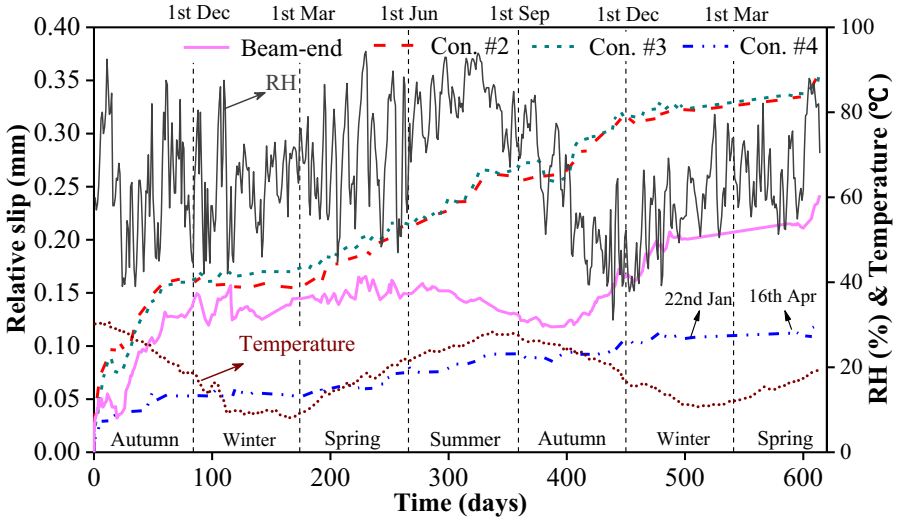

Fig. 8. Relative slips of specimen TCC-1.

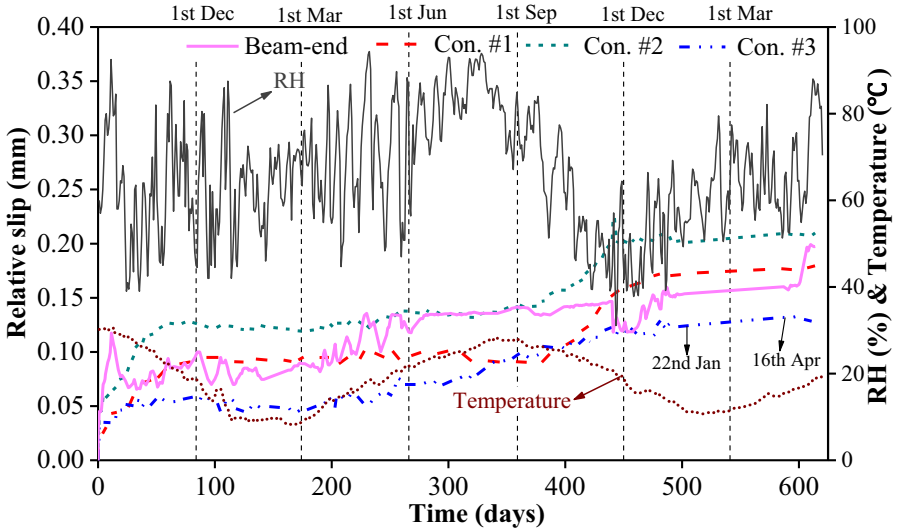

Fig. 9. Relative slips of specimen TCC-2.

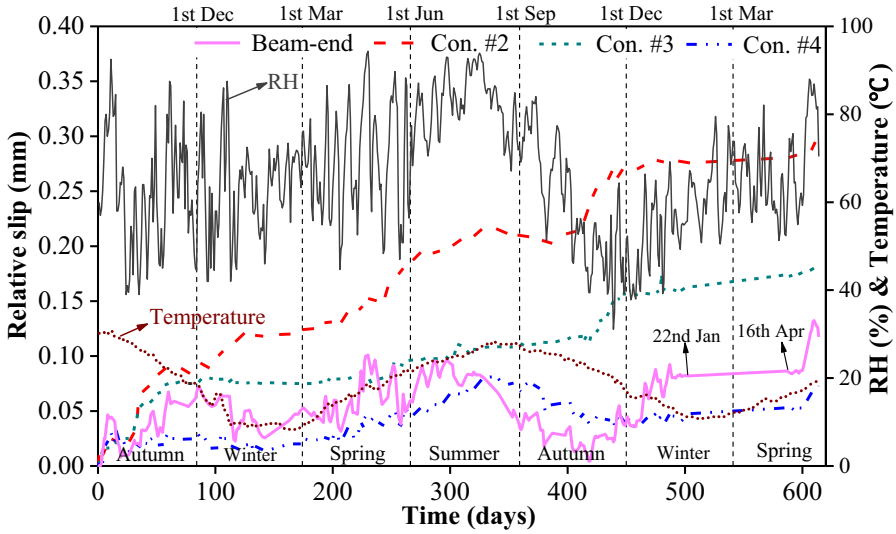

Fig. 10. Relative slips of specimen TCC-3.

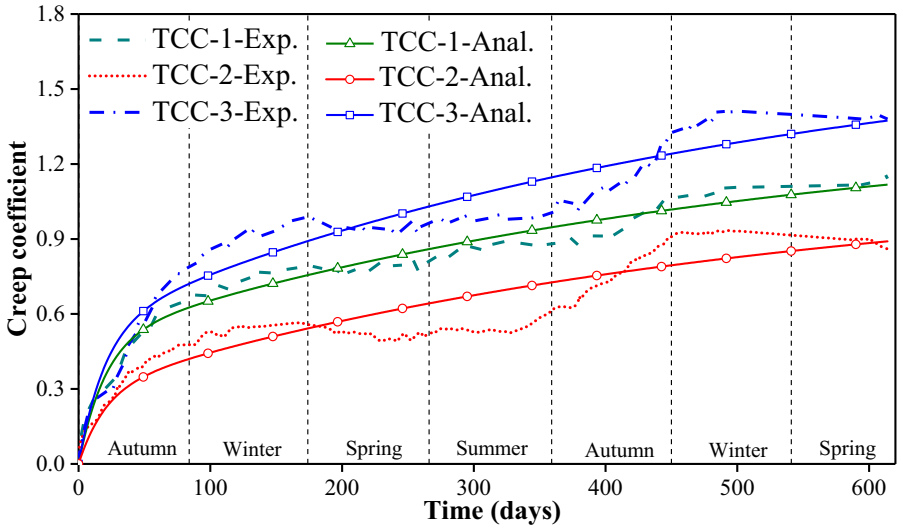

Fig. 11. Creep coefficients of mid-span deflections.

ulated by similar creep models, and the range of fluctuation was obviously smaller than the creep increment [34]. Thus, it was supposed that the creep models are effective tools to simulate the curves of creep coefficient [34,54].

$$\varphi(t) = J_1\left[1 - \exp\left(-\frac{t}{t_1}\right)\right] + J_2\left[1 - \exp\left(-\frac{t}{t_2}\right)\right] \quad (12)$$

where, J_1 and J_2 are the undetermined coefficients of the rheological model, t_1 and t_2 are the temporal intervals; t_1 = 20 days and t_2 = 500 days are adopted in this study.

The analytical fitting results according to Eq. (12) are plotted in Fig. 11. The undetermined parameters and R^2-values of two Kelvin bodies' model are shown in Table 8. It can be found the two Kelvin bodies' model can fit well the experimental results with the biggish values of R^2. As displayed in Fig. 11, the creep coefficients of mid-span deflections for all specimens fluctuated up and down with the seasonal cycle around the fitting curves. While the Kelvin model was used to predict the deformation of the specimens in the whole service life, the seasonal fluctuation will be ignored. This is because the deformation caused by seasonal variation of the RH and temperature also showed obvious seasonal fluctuation as shown in Fig. 11.

Table 8
Constitutive parameters and R^2 of two Kelvin bodies' model.

Specimen	J_1	J_2	R^2
TCC-1	0.536	0.733	0.983
TCC-2	0.367	0.568	0.890
TCC-3	0.623	0.889	0.960

4.2. Prediction of the mid-span deflection

The rheological creep model of Eq. (12) can be used to simply predict the long-term deformation in the whole service life. Based on the constitutive parameters in Table 8, the final deflections over the 50-year period were evaluated to be approximately 2.1~2.7 times initial deflections. The specific creep coefficients were estimated as 1.37 for specimen TCC-1, 1.14 for TCC-2 and 1.71 for TCC-3. The TCC structures with the fabricated shear connections

showed commendable long-term behaviour. Accordingly as shown in Table 9, the final deflections of each specimen at the end of 50-year service life are estimated as 13.63 mm, 13.31 mm and 7.80 mm, respectively.

Eurocode 5 [51] provides a simplified method to calculate the influences of load-duration and moisture on the long-term deformations of structures. In the serviceability limit state, the final deformation can be calculated by considering the modified elasticity of timber and concrete, and modified slip modulus of shear connection, as shown in Appendix Eqs. (13)–(15), respectively. For the timber component, the values of $k_{w,def}$ are given according to different service classes, i.e. 0.6 for service class 1, 0.8 for class 2, and 2.0 for class 3. The creep coefficient of concrete are influenced by many factors, including strength class, ambient RH and theoretical thickness of concrete section. For the concrete with an average compressive strength of 38.8 MPa, the creep coefficient $k_{c,def}$ is evaluated as 1.6 according to Eurocode 2 [47]. The shear connection of TCC structures is constituted of two components, having different time-dependent behaviours. Thus, the modified slip modulus $k_{s,def}$ should be calculated by Appendix Eq. (16). Substituting Eqs. (13)–(15) to the formula of effective bending stiffness Eq. (1), the final mid-span deflection at the end of 50-year can be calculated by Eq. (5).

Table 8 shows the final mid-span deflections at the end of service life (50 years) for all specimens. The final values of deflection predicted by Kelvin's model are between the results at service class 2 and those at service class 3 which conformed to the actual situation that the surrounding RH of all specimens were frequently at high levels exceeding 80%. This also demonstrated the reliability and accuracy of the Kelvin's model adopted.

4.3. Feasibility of the TCC beam with fabricated connections

The fabricated shear connection with lateral screws has been verified to exhibit pronounced bearing capacity, slip moduli and ductility, as shown in Table 3. The bending stiffness for a 6000 mm long TCC beam with 10 steel plate connections reaches to 9.16×10^{12}N.mm^2 (shown in Table 4), corresponding to a composite efficiency of 72%. Therefore, the TCC beam with the fabricated connections is acceptable and feasibility in terms of short-term structural performance.

The deflections of all specimens at different times are summarised at Table 10. Under the action of long-term loads (20% of static collapse capacity), the total deflection at the 613th day and at the end of service life are 12.31 and 13.63 mm for the specimen TCC-1, respectively, which were approximately 1/365 and 1/330 L_0 (net span), respectively. The creep coefficients at the end of record date (613 days) were 0.86 to 1.38. The final creep coefficients for the tested specimens are predicted as 1.14 to 1.71. During the 613-day of long-term tests, all specimens showed no deterioration, with superior state of sustaining loadings. Therefore, the experimental and predicted results demonstrated that the prefabricated TCC beam with steel plate connections showed acceptable long-term performance.

In addition, the short- and long-term performance of TCC beam could be optimized through further calculation coupled with practical engineering background. In conclusion, the prefabricated TCC beam with this type fabricated connection showed excellent short- and long-term structural performances, which was characterized by reliable bending stiffness, sufficient bearing capacity and eligible creep coefficient.

Table 10
The deflections of all specimens at different key times (Unit: mm).

Designations	TCC-1	TCC-2	TCC-3
Initial deflection	5.75	6.22	2.88
Total deflection at the 613th day	12.31	11.57	6.85
Final deflection	13.63	13.31	7.80

5. Conclusions

This article presented the experimental results about long-term performance of prefabricated TCC beams using steel plate connections. The long-term loading levels, the number of shear connections and environment factors (RH and temperature) are considered. Main discoveries can be concluded as follows:

(1) For the specimens TCC-1 and TCC-2 that sustained 20% of static bearing capacity, the increase in deflection are 6.56 and 5.35 mm after 613-day of loading. The specimen TCC-3 with the 0.10 loading level showed the deflection increment of 3.97 mm.
(2) The creep coefficients of all specimens were tested as 0.86–1.38 after 613-day of loading, and was estimated as 1.14–1.71 by the Kelvin's model after 50 years. The prefabricated TCC systems using this steel plate connections showed good long-term performance, demonstrating this type of shear connection exhibits the significant feasibility of application in engineering practice.
(3) While the long-term load was doubled, the deflection increment increases by about 60%. Conversely, the creep coefficient reduced by approximately 20%. With the increase of sustained loads, the creep deformation of the specimen did not develop linearly coupled with the long-term loads. Increasing sustained load led to the decline of the creep coefficient.
(4) The timber strain and beam-end slip showed stronger environmental sensitivity than deflections and relative slips at the positions of shear connections. The specimens with more shear connections exhibited slighter fluctuations with the vibration of surrounding RH and temperature.
(5) The decrease in air RH and temperature will cause the increase in deformation. The measured creep coefficient curves fluctuated up and down around the predicted ideal curve of the Kelvin model as the result of seasonal cycle of the surrounding environment.

Further investigation will focus on improving the creep models to consider the influence of periodic variation of RH and temperature. In addition, To decrease the creep deformation of steel-plate connections and corresponding TCC beams, the configuration of

Table 9
The final deflections predicted of all specimens (Unit: mm).

Specimens	Service class (Eurocode 5)			Prediction values by Kelvin model
	Service class 1	Service class 2	Service class 3	
TCC-1	11.16	12.38	17.39	13.63
TCC-2	11.78	13.09	18.75	13.31
TCC-3	5.58	6.19	8.70	7.80

steel-plate connections also can be further improved, through by providing a groove for the steel-plate on the timber, using bolts instead of screw, and adopting built-in type steel-plate connections.

CRediT authorship contribution statement

Benkai Shi: Writing - original draft. **Weiqing Liu:** Supervision, Methodology, Writing - review & editing. **Huifeng Yang:** Conceptualization, Methodology, Writing - review & editing.

Declaration of Competing Interest

The authors declare that they have no known competing financial interests or personal relationships that could have appeared to influence the work reported in this paper.

Acknowledgment

This work was supported by National Natural Science Foundation of China (Grant No. 51878344, 51578284), which are highly appreciated.

Appendix

This appendix presents the available theoretical formulas to evaluate the mid-span deflection, bending capacity of TCC beam specimens and the micro-stain of timber component. Also the modified elasticities of timber and concrete as well as the modified slip modulus suggested by Eurocode 5 [51] are displayed.

1. The effective bending stiffness can be calculated in accordance with Eurocode 5 [50] as Eqs. (1)–(4).

$$(EI)_{\text{eff}} = E_c I_c + E_w I_w + \gamma E_c A_c a_c^2 + E_w A_w a_w^2 \tag{1}$$

$$\gamma = \frac{1}{1 + \frac{\pi^2 E_c A_c S_s}{K_s L^2}} \tag{2}$$

$$a_w = \frac{\gamma E_c A_c (h_c + h_w)}{2(\gamma E_c A_c + E_w A_w)} \tag{3}$$

$$a_c = \frac{h_c + h_w}{2} - a_w \tag{4}$$

in which, subscripts *c* and *w* represent concrete and timber, respectively; *E*, *I*, *A* and *h* mean elastic modulus, inertia moment, section area and height, respectively; s_s and K_s mean the average distance and slip modulus of shear connections, respectively.

Accordingly, the mid-span deflection of a composite beam under the action of two equal concentrated loads arranged with equal intervals can be calculated by Eq. (5).

$$w = \frac{23PL^3}{1296(EI)_{\text{eff}}} \tag{5}$$

in which, *P* is the total experimental load.

2. For the TCC beam with non- and full-composite cation, the corresponding bending stiffness can be calculated by Eqs. (6) and (7), respectively.

$$(EI)_{\text{non}} = E_c I_c + E_w I_w \tag{6}$$

$$(EI)_{\text{full}} = E_c I_c + E_w I_w + E_c A_c a_c^2 + E_w A_w a_w^2 \tag{7}$$

To make comparisons with the slope of the bending test curve, the bending stiffness can be transformed to the stiffness *K* (N/mm) as suggested by Khorsandnia et al. [7].

$$K = \frac{P}{w} = \frac{1296EI}{23L^3} \tag{8}$$

The concept of 'composite efficiency' [55] was adopted to describe the composite action of shear connection, as illustrated by Eq. (9):

$$\phi = \frac{w_{\text{non}} - w_{\text{exp}}}{w_{\text{non}} - w_{\text{full}}} \tag{9}$$

in which, w_{non} and w_{full} is the theoretical full- and non-composite deflection, respectively. w_{exp} is the measured deflection of the specimen with incomplete composite action.

3. For the TCC beam with the T-shape section, the dominant failure mode is the bending failure of the timber beam. Therefore, the bearing capacity of TCC specimens can be calculated by Eq. (10) [39].

$$M_u = \frac{(EI)_{\text{eff}} f_m}{E_w h_e} \tag{10}$$

in which, f_m is the bending strength of timber, $h_e = h_w/2 + a_w$, and the slip moduli $K_{0.8}$ was recommended to calculate the $(EI)_{\text{eff}}$ at the collapse state.

4. Considering the effect of long-term load duration as well as surrounding RH and temperature of specimens, the elasticity of modulus for timber and concrete, and the slip stiffness of shear connection should be modified as the expression of Eqs. (13)–(15), respectively [51]. The modified coefficient of shear connection $k_{s,\text{def}}$ could be estimated by considering two components, as shown in Eq. (16).

$$E_{w,\text{fin}} = \frac{E_w}{1 + k_{w,\text{def}}} \tag{13}$$

$$E_{c,\text{fin}} = \frac{E_c}{1 + k_{c,\text{def}}} \tag{14}$$

$$K_{s,\text{fin}} = \frac{K_s}{1 + k_{s,\text{def}}} \tag{15}$$

$$k_{s,\text{def}} = 2\sqrt{k_{w,\text{def}} \cdot k_{c,\text{def}}} \tag{16}$$

References

[1] W. Liu, H. Yang, Research progress of modern wood structures, J. Build. Struct. 40 (02) (2019) 16–43 (in Chinese).
[2] A. Ceccotti, Composite concrete-timber structures, Progress Struct. Eng. Mater. 4 (3) (2002) 264–275.
[3] B.H. Ahmadi, M.P. Saka, Behavior of composite timber-concrete floors, J. Struct. Eng. 119 (11) (1993) 3111–3130.
[4] E. Steinberg, R. Selle, T. Faust, Connectors for timber-lightweight concrete composite structures, J. Struct. Eng. 129 (11) (2003) 1538–1545.
[5] J.L. Fernandez-Cabo, F. Arriaga, A. Majano-Majano, G. Iñiguez-González, Short-term performance of the HSB® shear plate-type connector for timber-concrete composite beams, Constr. Build. Mater. 30 (2012) 455–462.
[6] W.M. Sebastian, M. Piazza, T. Harvey, T. Webster, Forward and Reverse shear transfer in beech LVL-concrete composites with singly inclined coach screw connectors, Eng. Struct. 175 (2018) 231–244.
[7] N. Khorsandnia, H.R. Valipour, K. Crews, Experimental and analytical investigation of short-term behaviour of LVL-concrete composite connections and beams, Constr. Build. Mater. 37 (2012) 229–238.
[8] D. Yeoh, M. Fragiacomo, M. De Franceschi, A.H. Buchanan, Experimental tests of notched and plate connectors for LVL-concrete composite beams, J. Struct. Eng. 137 (2) (2011) 261–269.
[9] L. Boccadoro, S. Zweidler, R. Steiger, A. Frangi, Bending tests on timber-concrete composite members made of beech laminated veneer lumber with notched connection, Eng. Struct. 132 (2017) 14–28.
[10] J.L. Miotto, A.A. Dias, Evaluation of perforated steel plates as connection in glulam-concrete composite structures, Constr. Build. Mater. 28 (1) (2012) 216–223.
[11] P.S. Clouston, S. Civjan, L. Bathon, Experimental behavior of a continuous metal connector for a wood-concrete composite system, Forest. Prod. J. 54 (6) (2004) 76–84.

[12] D.D. Djoubissie, A. Messan, E. Fournely, A. Bouchaïr, Experimental study of the mechanical behavior of timber-concrete shear connections with threaded reinforcing bars, Eng. Struct. 172 (2018) 997–1010.
[13] M.R. LeBorgne, R.M. Gutkowski, Effects of various admixtures and shear keys in wood-concrete composite beams, Constr. Build. Mater. 24 (9) (2010) 1730–1738.
[14] F. Suárez-Riestra, J. Estévez-Cimadevila, E. Martín-Gutierrez, D. Otero-Chans, Perforated shear + reinforcement bar connectors in a timber-concrete composite solution. Analytical and numerical approach, Compos. Part B: Eng. 156 (2019) 138–147.
[15] A. Ceccotti, M. Fragiacomo, S. Giordano, Behaviour of a timber–concrete composite beam with glued connection at strength limit state, Proceedings 9th World Conference on Timber Engineering (WCTE 2006), Portland, Oregon, USA, 2006.
[16] E. Lukaszewska, M. Fragiacomo, H. Johnsson, Laboratory tests and numerical analyses of prefabricated timber-concrete composite floors, J. Struct. Eng. 136 (1) (2009) 46–55.
[17] E. Lukaszewska, H. Johnsson, M. Fragiacomo, Performance of connections for prefabricated timber-concrete composite floors, Mater. Struct. 41 (9) (2008) 1533–1550.
[18] R. Crocetti, T. Sartori, R. Tomasi, Innovative timber-concrete composite structures with prefabricated FRC slabs, J. Struct. Eng. 141 (9) (2014) 04014224.
[19] N. Khorsandnia, H. Valipour, J. Schänzlin, K. Crews, Experimental investigations of deconstructable timber-concrete composite beams, J. Struct. Eng. 142 (12) (2016) 04016130.
[20] W. Zhu, H. Yang, W. Liu, B. Shi, Z. Ling, H. Tao, Experimental investigation on innovative connections for timber-concrete composite systems, Constr. Build. Mater. 207 (2019) 345–356.
[21] Y. Zhang, G.M. Raftery, P. Quenneville, Experimental and analytical investigations of a timber-concrete composite beam using a hardwood interface layer, J. Struct. Eng. 145 (7) (2019) 04019052.
[22] L.F.C. Jorge, S.M.R. Lopes, H.M.P. Cruz, Interlayer influence on timber-LWAC composite structures with screw connections, J. Sruct. Eng. 137 (5) (2010) 618–624.
[23] M. Fragiacomo, E. Lukaszewska, Development of prefabricated timber–concrete composite floor systems, Proc. Inst. Civ. Eng.: Struct. Build. 164 (2) (2011) 117–129.
[24] M. Fragiacomo, J. Schänzlin, Proposal to account for concrete shrinkage and environmental strains in design of timber-concrete composite beams, J. Struct. Eng. 139 (1) (2012) 162–167.
[25] A.M.P.G. Dias, J.W.G. Van de Kuilen, S. Lopes, H. Cruz, A non-linear 3D FEM model to simulate timber-concrete joints, Adv. Eng. Softw. 38 (8–9) (2007) 522–530.
[26] L. Eisenhut, W. Seim, S. Kühlborn, Adhesive-bonded timber-concrete composites-Experimental and numerical investigation of hydrothermal effects, Eng. Struct. 125 (2016) 167–178.
[27] J.W.G. Van de Kuilen, A.M.P.G. Dias, Long-term load-deformation behaviour of timber-concrete joints, Proc. Inst. Civ. Eng.: Struct. Build. 164 (2) (2011) 143–154.
[28] M. Fragiacomo, C. Amadio, L. Macorini, Short-and long-term performance of the "Tecnaria" stud connector for timber-concrete composite beams, Mater. Struct. 40 (10) (2007) 1013–1026.
[29] A. Ceccotti, M. Fragiacomo, S. Giordano, Long-term and collapse tests on a timber-concrete composite beam with glued-in connection, Mater. Struct. 40 (1) (2007) 15–25.
[30] L. To, M. Fragiacomo, J. Balogh, R.M. Gutkowski, Long-term load test of a wood-concrete composite beam, Proc. Inst. Civ. Eng.: Struct. Build. 164 (2) (2011) 155–163.
[31] T. Tannert, B. Endacott, M. Brunner, T. Vallée, Long-term performance of adhesively bonded timber-concrete composites, Int. J. Adhes. Adhes. 72 (2017) 51–61.
[32] R.M. Gutkowski, N.J. Miller, M. Fragiacomo, J. Balogh, Composite wood-concrete beams using utility poles: time-dependent behavior, J. Struct. Eng. 137 (6) (2010) 625–634.
[33] J. Kanócz, V. Bajzecerová, Influence of rheological behaviour on load-carrying capacity of timber-concrete composite beams under long term loading, Procedia Eng. 40 (2012) 20–25.
[34] D. Yeoh, K.H. Boon, L.Y. Loon, Timber-concrete composite floor beams under 4 years long-term load, Int. J. Integr. Eng. 5 (2) (2013) 1–7.
[35] M. Fragiacomo, E. Lukaszewska, Time-dependent behaviour of timber-concrete composite floors with prefabricated concrete slabs, Eng. Struct. 52 (2013) 687–696.
[36] V. Bajzecerová, J. Kanócz, The effect of environment on timber-concrete composite bridge deck, Procedia Eng. 156 (2016) 32–39.
[37] M. Fragiacomo, R.M. Gutkowski, J. Balogh, R.S. Fast, Long-term behavior of wood-concrete composite floor/deck systems with shear key connection detail, J. Struct. Eng. 133 (9) (2007) 1307–1315.
[38] M. Fragiacomo, E. Lukaszewska, Influence of the construction method on the long-term behavior of timber-concrete composite beams, J. Struct. Eng. 141 (10) (2015) 04015013.
[39] B. Shi, W. Zhu, H. Yang, W. Liu, H. Tao, Z. Ling, Experimental and theoretical investigation of prefabricated timber-concrete composite beams with and without prestress, Eng. Struct. 204 (2020) 109901.
[40] CEN, Timber structures – Glued laminated timber – Strength classes and determination of characteristic values, EN 1194. Brussels, 1999.
[41] ASTM D198-02, Standard test methods of static tests of lumber in structural sizes. American Society for Testing and Materials, 2002.
[42] Ministry of Housing and Urban-Rural Development of the People's Republic of China (MOHURD). GB/T 50329-2012: Standard for test methods of timber structures. China Building Industry Press, 2012 [in Chinese].
[43] ISO 3347: 1976, Wood-Determination of ultimate shearing stress parallel to grain, 1976.
[44] ISO 3345: 1975, Wood-Determination of ultimate tensile stress parallel to grain, 1975.
[45] ASTM D905-08(2013), Standard test methods of strength properties of adhesive bonds in shear by compression loading. American Society for Testing and Materials, 2013.
[46] CEN, Moisture content of a piece of sawn timber – Part 1: Determination by oven dry method, EN 13183-1. Brussels, 2002.
[47] CEN, Eurocode 2: Design of concrete structures – Part 1: General rules and rules for buildings, EN 1992-1-1. Brussels, 2004.
[48] ASTM F1575-17, Standard test method for determining bending yield moment of nails. American Society for Testing and Materials, 2017.
[49] CEN, Timber Structures – Test methods – Withdrawal capacity of timber fasteners, EN 1382. Brussels, 2016.
[50] B. Shi, W. Liu, H. Yang, X. Ling, Long-term performance of timber-concrete composite systems with notch-screw connections, Eng. Struct. 213 (2020) 110585.
[51] CEN, Eurocode 5: Design of timber structures – Part 1-1: General – Common rules and rules for buildings, EN 1995-1-1. Brussels, 2004.
[52] B. Shi, H. Yang, J. Liu, R. Crocetti, W. Liu, Short-and long-term performance of bonding steel-plate joints for timber structures, Constr. Build. Mater. 240 (2020) 117945.
[53] W.G. Davids, H.J. Dagher, J.M. Breton, Modeling creep deformations of FRP-reinforced glulam beams, Wood Fiber Sci. 32 (4) (2000) 426–441.
[54] Q. Xu, L. Chen, K.A. Harries, F. Zhang, Z. Wang, X. Chen, Experimental study and numerical simulation of long-term behavior of timber beams strengthened with near surface mounted CFRP bars, Mater. Struct. 50 (1) (2017) 45.
[55] R.M. Gutkowski, W. Thompson, K. Brown, P. Etournaud, A. Shigidi, J. Natterer, Laboratory tests of composite wood-concrete beam and deck specimens, in: Proceedings of 1999 RILEM Symposium on Timber Engineering, 1999, pp. 263–272.